

Lévy statistical fluctuations from a Random Amplifying Medium

Divya Sharma, Hema Ramachandran and N. Kumar

Raman Research Institute, Sadashivanagar, Bangalore 560 080, India.

Abstract

We report the studies of emission from a novel random amplifying medium that we term a “Lévy Laser” due to the non-Gaussian statistical nature of its emission over the ensemble of random realizations. It is observed that the amplification is dominated by certain improbable events that are “larger than rare”, which give the intensity statistics a Lévy like “fat tail”. This, to the best of our knowledge, provides the first experimental realization of Lévy flight in optics in a random amplifying medium.

1 Introduction

Random variables having orders-of-magnitude large values, but with correspondingly orders-of-magnitude small probabilities for their occurrence, are known to give non-Gaussian statistics for their fluctuations - the Lévy statistics [1]. For these *larger-than-rare* events the variance diverges, and a single large event may typically dominate the sum of large number of such random events. Many physical examples of Lévy statistics, or the Lévy flights, are realized in nature, for example, strange kinetics [2], anomalous diffusion in living polymers [3], subrecoil laser cooling [4], rotating fluid flow [5] and interstellar scintillations [6].

In the present work a Random Amplifying Medium (RAM) is shown to provide yet another example of Lévy statistics of some physical interest. In a RAM, light scattering, which is usually considered detrimental to laser action, can in fact, lead to enhanced amplification and hence to lasing. Here we report some analytical and experimental results on the anomalous fluctuations of emission from a RAM pumped beyond a threshold of gain. More specifically, we show that in the classical diffusive regime, as obtaining in our systems, there is a crossover from the Gaussian to the Lévy statistics for the emission intensity over the ensemble of realizations of the random medium. Also, the associated Lévy exponent decreases with the increasing gain. An interesting finding is that the Lévy-statistical fluctuations are enhanced by embedding an amplifying fiber into the particulate RAM. We also briefly discuss the nature of these fluctuations as distinct from those observed in transport through passive random media.

A RAM normally consists of an active bulk medium, like an optically pumped laser dye solution (for example Rhodamine in methanol) in which point-like (particulate) scatterers (rutile (TiO_2) or polystyrene microspheres) are randomly suspended [7-17]. Unlike the case of a conventional laser with external cavity mirrors providing resonant feedback,

in a RAM it is the multiple scattering of light that provides a non-resonant distributed feedback (Fig 1), and hence the mirrorless lasing. The enhanced path-lengths within the random medium may arise due to classical diffusion resulting from incoherent scattering (dilute suspension of scatterers in a dye) [8-12,16], or due to incipient wave localization with strong coherent scattering (for example semiconductor powder ZnO, GaN) [13-15]. In general, in a RAM operating in the incoherent diffusive regime, greater the refractive-index mismatch, greater is the diffusive path-length enhancement, and hence greater the amplification. A clear signature of lasing in a RAM is the drastic spectral narrowing (gain narrowing) of the emission from the system above a well defined threshold of pump power. In the dye-scatterer system, the threshold of the pump power, at which the emission linewidth collapses from a few tens of nanometer to a few nanometers, is almost two orders of magnitude smaller in the system with scatterers than the one without. Further, with the increase in the scatterer concentration, both, the linewidth and the pumping threshold are observed to decrease drastically. The selection of the lasing wavelength, however, arises here as a result of an optimization involving, for example, the wavelength-dependent diffusion coefficient (or the localization length scale) and the spectral profile of the pumped dye.

An important aspect of the random lasing is that for a high gain (pumping) the randomness of the amplifying medium makes the emission fluctuate strongly over the different microscopic realizations (complexions) of the randomness of the medium. This shows up as non-self averaging fluctuations of the observed lasing intensity as the medium is varied over its random realizations, for example, by tapping the cuvette containing the RAM. (This, of course, is quite different from the inherent photon statistics of fluctuations in time observed for a given complexion [17]). Normally, i.e., for passive random media, these “sample-to-sample” fluctuations are Gaussian in nature. In this work we will be concerned with fluctuations in a RAM only.

To fix the idea, consider a RAM with the scatterers dispersed densely and randomly in an amplifying continuum. A spontaneously emitted photon is expected to diffuse with a diffusion constant $D = (1/3)c\ell$, where ℓ is the elastic mean free path and c is the speed of light in the medium. We assume classical diffusion as $\ell/\lambda \gg 1$ in our case, where, λ is the optical wavelength. As the photon diffuses and eventually escapes, it undergoes amplification, or gain (multiplication) due to the optical pumping, and the associated stimulated emission, which, of course, does not affect D . Assuming for simplicity, a spherical RAM (radius ‘ a ’), illuminated uniformly by a short pump-pulse at time $t = 0$, the probability of escape of a photon from the surface at $r = a$, per unit time at time t is given by (the first-passage probability density)

$$p_I(t) = -\frac{\partial}{\partial t} \int_0^a \rho(r, t) 4\pi r^2 dr , \quad (1)$$

where, $\rho(r, t)$ is the probability density of the diffusing photon, emitted spontaneously at time $t = 0$ anywhere within the sample with a uniform initial probability density (ρ_0). Simple solution for the diffusion problem (with the absorbing boundary condition at $r = a$) gives

$$\rho(r, t) = \rho_0 \sum_{m=1}^{\infty} \left(\frac{2a}{\pi m}\right) (-1)^{m+1} \cdot \frac{\sin(\pi m r/a)}{r} e^{-\frac{\pi^2 m^2}{a^2} D t} \quad (2)$$

giving straightforwardly

$$p_I(t) = \rho_0 \sum_{m=1}^{\infty} 8aDe^{-\frac{\pi^2 m^2}{a^2}Dt} \quad (3)$$

Now, the arc path-length traversed in the diffusion time t is ct giving a gain factor $g = e^{ct/\ell_g}$, where ℓ_g is the gain length for the RAM. This at once gives, with change of variable, the probability distribution for the gain $p_g(g)$ as

$$p_g(g) = \sum_{m=1}^{\infty} \left(\frac{\rho_0 8aD\ell_g}{c} \right) \frac{1}{g^{1+\alpha_m}} \equiv \sum_{m=1}^{\infty} \left(\frac{8\rho_0}{3} \right) (a\ell_g) \frac{1}{g^{1+\alpha_m}} \quad (4)$$

with $\alpha_m = m^2(\frac{\pi^2 \ell_g}{a^2}) \equiv$ the m^{th} Lévy exponent. Thus, with increasing pumping (decreasing gain length ℓ_g), the exponent α_m decreases, the tail becomes fatter, and the variance of g diverges for $\alpha_m < 2$, that happens first for $m = 1$, i.e., for $(\frac{\pi^2 \ell_g}{a^2}) < 2$. This leads to the crossover from a finite variance (Gaussian) to a divergent variance (Lévy) limit. This essentially describes the onset of Lévy fluctuations as we increase optical pumping. It is idealized in that only the photons spontaneously emitted at time $t = 0$ are considered. These are amplified most anyway, and dominate the intensity at time t observed, for large gains (high pump powers). Further, in our granular random media with grain size $\gg \lambda$, the random scattering is best described as random refractions at the interfaces. This can give rise to random closed loops that can trap and enhance light as in a resonance. Also, inasmuch as the escape rate is linked to the diffusion constant, one can expect the classical Ruelle-Pollicott resonances giving pronounced structure to the fluctuation statistics. We have not addressed these issues here.

Before we proceed further (with experiments), let us clarify the meaning of “*fluctuations*” once more in our context. These are statistical fluctuations over the ensemble of realizations of the randomness (i.e., macroscopically identical RAMs). Of course, we can invoke physically the idea of ergodicity and identify these fluctuations as unfolding in different parametric contexts. Statistical fluctuations of transmission/conductance through passive random media are, of course, well known [18], where, for a macroscopic sample, the classical fluctuations are small relative to the wave-mechanical (or quantum) fluctuations due to coherent interference effects. In the present case of strictly classical diffusion ($\ell \gg \lambda$), the anomalously large fluctuations are due entirely to the amplification inherent to a RAM.

The system that we have experimentally studied is a novel RAM, which we term the F-RAM (Fiber-Random Amplifying Medium), inasmuch as the active medium is a random aggregation of segments of dye-doped amplifying (one-dimensional) fibers (Bicron, red fluorescent optical fiber) in a passive medium of air, granular starch etc. (Fig 2). These plastic fibers fluoresce in the orange-red when pumped by green light that enters the fibers through their cylindrical surfaces anywhere along their lengths. The emitted fluorescent light is mainly guided along the length, and it emerges from either end amplified by a factor that increases exponentially with the length of travel through the fiber. While the random aggregation of the amplifying fibers itself provides some scattering, the latter was enhanced in our experiments by the addition of passive scatterers like non-active fiber pieces or granular starch. Thus, the diffusion proceeds via random scattering and wave-guidance.

Our initial experiments studied the emission from an F-RAM, made of amplifying fibers crushed to sub-millimeter sizes, both with and without long pieces of amplifying

fibers embedded in it. Additionally, these were compared with an F-RAM consisting of long pieces of amplifying fibers embedded in a passive scattering medium. These experiments and the observations are described in section 2. The Arrhenius cascade model as also the Lévy microscope [19], to which the observed statistics of intensity fluctuations bear relevance, is described in section 3. The experimental realization of Lévy lasers, i.e., F-RAMs with tailored length distribution, exhibiting the sample-to-sample Lévy intensity fluctuations, in the dilute and the dense limits, is described in section 4. Section 5 concludes the work.

2 Experiments in F-RAM

An F-RAM consisting of amplifying fibers crushed to sub-millimeter sizes (which serve both to amplify and scatter the light), was contained in a glass cuvette of size 1 cm×1 cm ×5 cm. This was pumped by 10 ns, 26 mJ pulses at 532 nm from a frequency doubled Nd:YAG laser (Spectra Physics). Part of the pump beam was split off by a beam-splitter to monitor the pump intensity that was maintained constant. The emission from the sample was collected transverse to the pump beam and the spectrum analyzed on a PC based spectrometer (Ocean Optics). The schematic of the experimental set-up is shown in Fig 3. Lasing action was seen from this system above a pump threshold of 22 mJ (Fig 4). The complexion of the system was altered i.e. the sample was agitated, so that different random configurations were obtained, and the resulting emission spectra were recorded. In order to obtain good statistics, this was repeated till the emission spectra for 420 different complexions of the sample were obtained. A histogram was then constructed; that is the probability $P(I)$ ¹ of obtaining intensity I was plotted as a function of the intensity. The histograms shown for $\lambda = 620 \text{ nm}$ (emission peak) and $\lambda = 590 \text{ nm}$ (off-peak) are both observed to be Gaussian (Fig 5(a,b)). The intensity as a function of complexion for these wavelengths show small fluctuations (Fig 5(c,d)).

Ten long pieces (length 6 mm) of amplifying fibers were then added to the above F-RAM, and in a similar fashion the spectra for 420 different complexions of the sample recorded. A typical spectrum of this F-RAM is shown in Fig 6. Unlike the earlier case, the histogram at $\lambda = 640 \text{ nm}$ (peak) shows a marked departure from the Gaussian in the form of a long fat tail (Fig 7(a)). In addition, the intensity as a function of complexion showed sudden large fluctuations (Fig 7(c)). In contrast, at $\lambda = 590 \text{ nm}$ (off-peak), the intensity fluctuations remained small (Fig 7(d)) and the histogram Gaussian (Fig 7(b)). The departure from the normally observed Gaussian statistics and the sudden large intensity fluctuations at the peak emission wavelength (640 nm) can be explained as arising from the few long pieces of amplifying fiber, that, in some complexions of the sample, provide large gain resulting in the fat tail. This was verified by studying another system that consisted of a passive scattering bulk medium (white fiber pieces, length $\sim 1 \text{ mm}$), in which five pieces of amplifying fiber (length 6 mm) were embedded, at pump energy of $\sim 12 \text{ mJ}$. The presence of the pieces of amplifying fiber, though not visually apparent, is evident from the intensity statistics of the emitted spectra as a long tail in the histogram at $\lambda = 640 \text{ nm}$ (Fig 8(a)) and corresponding large intensity fluctuations over different complexions (Fig 8(c)). On the other hand, the histogram and the intensity fluctuations at $\lambda = 590 \text{ nm}$ (Figs 8(b,d)) show Gaussian statistics. It is thus clear that

¹ $P(I)$ is the number of times an intensity was recorded normalized to the total number of spectra.

a few long pieces of amplifying fiber dominate the emission by their large, but rare, amplification so much so that the presence of a few long amplifying pieces hidden inside a bulk aggregate of small pieces (active or passive) can be inferred from the sample-to-sample fluctuations in the emission from the system. This feature may be used to probe a relatively long piece of amplifying fiber hidden inside a RAM thus Lévy microscope ².

3 The Arrhenius cascade

As the above experiments on F-RAMs indicate that a few large events dominate the emission statistics, we are led to the related problem of the Arrhenius cascade, which we discuss in brief. The Arrhenius cascade studies the time of descent of a particle down an incline that has a series of potential wells of varying random depths, U , occurring with probability $p_U(U) = \frac{1}{U_o} \exp(-\frac{U}{U_o})$ (U_o is the mean depth) (Fig 9(a): dotted). In a well of depth U , the particle spends a time t , with $\tau = \frac{t}{t_o} = \exp(\frac{U}{kT})$ (Fig 9(a): solid). Thus, though deep wells are exponentially improbable, their presence increases the residence time exponentially. It can be shown that in the asymptotic limit, the total time of descent follows the power law $p_\tau(\tau) \sim \tau^{(-1-\alpha)}$ where, $\alpha = \frac{kT}{U_o}$. For high temperature (T), or for $\alpha \geq 2$, the particle has a fast descent and the resulting distribution $p_\tau(\tau)$ is Gaussian. For $0 < \alpha < 2$, corresponding to intermediate or low temperatures, the distribution is Lévy (Fig 9(b)) and the Central Limit Theorem is violated.

To exploit the fact that two functions, one exponentially increasing and the other exponentially falling, can combine to give rise to Gaussian or Lévy statistics depending on the relative values of the two exponents, we tailored our F-RAM system, such that the probability distribution of the lengths of the fibers was $p_\ell(\ell) = \frac{1}{\ell_o} \exp(-\frac{\ell}{\ell_o})$, as shown in Fig 10. (Note that this tailored F-RAM is different from those described in section 2 where all long amplifying fiber pieces were of same length). The amplification within an active fiber results in an intensity $I(\ell) = I_o \exp(\frac{\ell}{\ell_g})$, or gain $g_\ell = \frac{I(\ell)}{I_o} = \exp(\frac{\ell}{\ell_g})$. Thus, long fibers, though exponentially rare, provide exponentially high gain ³.

It can be shown that the probability distribution of the resultant gain acquired by the photon is given as $p_g(g) \sim g^{(-1-\nu)}$ where, $\nu = \frac{\ell_g}{\ell_o}$. It is thus expected that $0 < \nu < 2$ gives Lévy intensity statistics and $\nu \geq 2$ Gaussian. We demonstrate experimentally, in the next section, the crossover from Gaussian to Lévy as ℓ_g is reduced.

4 Experiments with tailored F-RAM (Lévy Laser)

Experiments were conducted on tailored F-RAMs with N pieces ($N = 350, 800$) of amplifying fibers in passive scattering media provided by suspension of polystyrene microspheres in water (BangsLabs, mean diameter = $0.13 \mu m$, number density = $9.357 \times 10^{12}/cc$), granular starch or pieces of white optical fiber (non-amplifying, length ~ 0.5 mm to 1 mm). In all three systems (contained in glass cuvettes of size 30 mm \times 30 mm \times 60 mm) were studied in which, the lengths of the amplifying fibers ranged from 1 mm to 20 mm and followed an exponential distribution with $\ell_o = 5$ mm.

²The term “Lévy microscope” will become clearer after section 3

³Note that the parameters ℓ_o and ℓ_g in the tailored F-RAM correspond to U_o and kT respectively in the Arrhenius cascade

As described in section 2, spectra (at pump energies $\sim 6\text{-}9$ mJ) for ~ 360 different complexions of each of the systems were obtained and analyzed. The intensity fluctuations and the corresponding histograms are given in Figs 11 to 13. These are shown for $\lambda = 645$ nm and 590 nm, the former corresponding to the peak emission wavelength, where the gain is maximum (ℓ_g is minimum), and the latter to off-peak wavelength (ℓ_g is large). The histograms of all three systems show a Lévy-like fat tail at the peak emission wavelength; therefore these tailored F-RAMs are termed Lévy lasers. In contrast, at off-peak wavelengths, the histograms show Gaussian statistics consistent with the larger value of ν . The intensity at the peak wavelength (645 nm) as a function of complexion showed sudden large jumps, typical of Lévy flights. This feature was absent at off-peak wavelengths.

We now distinguish between the “dilute” and the “dense” limits of the Lévy Laser. The dilute Lévy Laser contains a few pieces of amplifying fibers. A photon originating within a given piece of amplifying fiber gains in intensity as it traverses the fiber. Upon exiting the fiber, it diffuses through the passive surrounding medium and exits the sample with a negligible probability of encountering another amplifying fiber (Fig 14(a)). The intensity collected in the experiment is the sum of various such intensities - the *additive gain*. As discussed earlier, it gives a power-law for the gain i.e., $p_g(g) \sim g^{-1-\nu}$. Of the systems studied, the case with $N = 350$ amplifying fibers in polystyrene scattering medium corresponds to a dilute system. The tail of the histogram can be fitted to a power law function ($g^{-1-\nu}$) with exponent $1 + \nu = 2.69$ i.e., $\nu = 1.69$.

In the dense Lévy laser, on the other hand, a photon, upon exiting an amplifying fiber, has a high probability of entering another amplifying fiber and getting further amplified before finally exiting the sample (Fig 14(b)). In such a case, the total intensity (or gain) is *multiplicative* rather than *additive* i.e. $G = \prod_i g_{\ell_i} = \prod_i \exp(\frac{\ell_i}{\ell_g})$, where, the index, i , runs over all fibers that a given photon traverses through, from which we get $p_x(x) \sim g^{-\nu}$ where, $x = \ln g_{\ell_i}$. Thus, the dense system with multiplicative gain also gives rise to a Lévy distribution, but with a tail that falls off slower than the dilute system. Cases with $N = 800$ amplifying fibers in passive scattering media are realizations of dense Lévy lasers. The tails of the histograms can be fitted to the power law function ($g^{-\nu}$) with exponents $\nu = 0.62$ and 1.68 , for systems with passive scattering medium as non-active white fiber pieces and granular starch respectively.

5 Conclusions

We have demonstrated a new RAM, namely the F-RAM, that is notably different from a conventional RAM in several aspects. As opposed to the RAM that has a bulk active medium (dye solution) with suspended passive point-like scatterers, an F-RAM, has an active medium that is one-dimensional (pieces of amplifying fiber) and is suspended in the passive bulk medium. Further, unlike the conventional RAM, during its traversal through the passive bulk medium in an F-RAM the photon does not get amplified. Consequently, a greater refractive index mismatch between the active (fiber) and the passive (bulk) media, which in the case of RAM leads to greater amplification due to increased path-length, is likely to result under some conditions in just the opposite in an F-RAM, as it enhances scattering off the active fiber. We term an F-RAM with a tailored distribution of fiber lengths, where long amplifying pieces are exponentially rare, a “Lévy Laser”, because the

sample-to-sample intensity fluctuations exhibit Lévy statistics. The “larger than rare” amplification in such systems makes feasible a “Lévy microscope” that can pick out the presence of, and study the characteristics of a long piece of amplifying fiber embedded in a bulk of smaller (active or passive) pieces.

References

- [1] Michael F. Shlesinger, George M. Zaslavsky and Uriel Frisch (Eds.), “Lévy flights and related topics in physics”, Lecture notes in physics, Vol. 450, (Springer-Verlag Berlin, Heidelberg) (1995).
- [2] Michael F. Shlesinger, George M. Zaslavsky and Joseph Klafter, “Strange kinetics”, *Nature* **363**, 31 (1993).
- [3] A. Ott, J.P. Bouchaud, D. Langevin and W. Urbach, “Anomalous diffusion in “living polymers”: A genuine Lévy flight?”, *Phys. Rev. Lett.* **65**, 2201 (1990).
- [4] F. Bardou, J.P. Bouchaud, O. Emile, A. Aspect and C. Cohen-Tannoudji, “Subrecoil laser cooling and Lévy flights”, *Phys. Rev. Lett.* **72**, 203 (1994).
- [5] T.H. Solomon, Eric R. Weeks and Harry L. Swinney, “Observation of anomalous diffusion and Lévy flights in a two-dimensional rotating flow”, *Phys. Rev. Lett.* **71**, 3975 (1993).
- [6] Stanislav Boldyrev and Carl R. Gwinn, “Lévy model for interstellar scintillations”, *Phys. Rev. Lett.* **91**, 131101 (2003).
- [7] For a comprehensive review, see “Localization, multiple scattering, and lasing in random nanomedia”, Stephen C. Rand, Costas Soukoulis and Diederik S. Wiersma (Eds.), *J. Opt. Soc. Am. B* **21**, 98 (2004), Special issue.
- [8] V.S. Letokhov, “Generation of light by a scattering medium with negative resonance absorption”, *Sov. Phys. JETP* **26**, 835 (1968).
- [9] N.M. Lawandy, R.M. Balachandran, A.S.L. Gomes and E. Souvain, “Laser action in strongly scattering media”, *Nature* **368**, 436 (1994).
- [10] Diederik S. Wiersma and Ad Lagendijk, “Light diffusion with gain and random lasers”, *Phys. Rev. E* **54**, 4256 (1996).
- [11] Sajeev John and Gendi Pang, “Theory of lasing in a multiple-scattering medium”, *Phys. Rev. A* **54**, 3642 (1996).
- [12] B. Raghavendra Prasad, Hema Ramachandran, Ajay Kumar Sood, C.K. Subramanian and Narendra kumar, “Lasing in active, sub-mean-free path-sized systems with dense, random, weak scatterers”, *Applied Optics* **36**, 7718 (1997).
- [13] H. Cao, Y.G. Zhao, S.T. Ho, E.W. Seelig, Q.H. Wang and R.P.H. Chang, “Random laser action in semiconductor powder”, *Phys. Rev. Lett.* **82**, 2278 (1999).

- [14] H. Cao, J.Y. Xu, S.-H. Chang and S.T. Ho, “Transition from amplified spontaneous emission to laser action in strongly scattering media”, *Phys. Rev. E* **61**, 1985 (2000).
- [15] Prabhakar Pradhan and N. Kumar, “Localization of light in coherently amplifying random media”, *Phys. Rev. B (Rapid Communications)*, **50**, 9644 (1994).
- [16] Sushil Mujumdar, Marilena Ricci, Renato Torre and Diederik S. Wiersma, “Amplified extended modes in random lasers”, *Phys. Rev. Lett.* **93**, 053903 (2004).
- [17] Giannis Zacharakis, Nektarios A. Papadogiannis, George Filippidis and Theodore G. Papazoglou, “Photon statistics of laserlike emission from polymeric scattering gain media”, *Optics Letters* **25**, 923 (2000).
- [18] For a general discussion of fluctuations of wave transmission, see “Quantum transport in mesoscopic systems : Complexity and statistical fluctuations”, P.A. Mello and N. Kumar, Oxford university press (London), *Mesoscopic physics and nanotechnology*, 4 (2004).
- [19] F. Bardou, “Cooling gases with Lévy flights: using the generalized central limit theorem in physics”, *arXiv:physics/ 0012049 v1*, 20 Dec 2000.

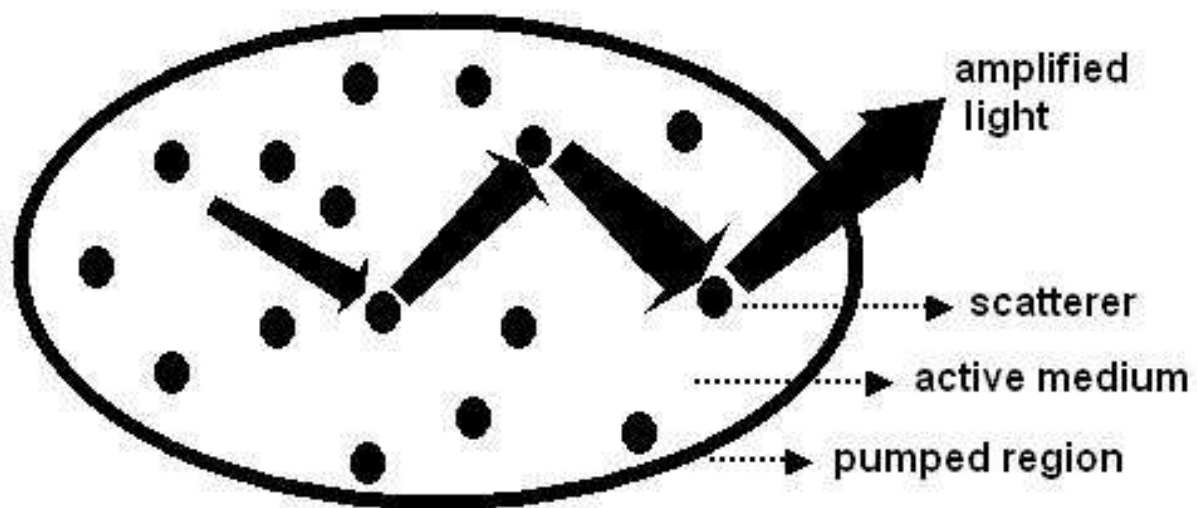


Figure 1: *Schematic of a RAM illustrating amplification due to multiple scattering.*

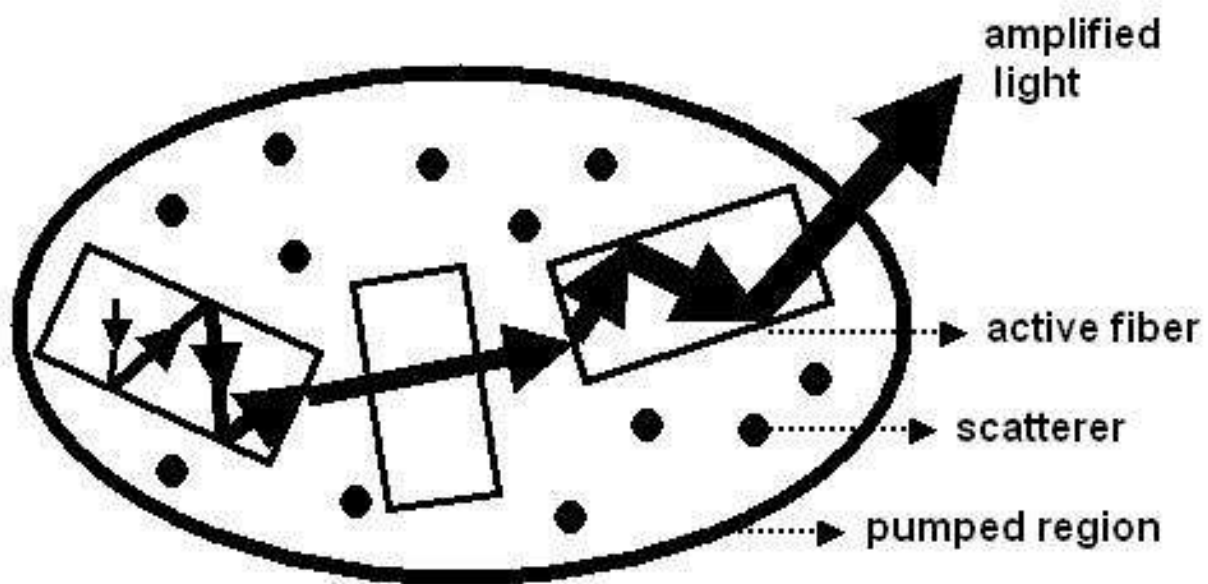


Figure 2: *Schematic of an F-RAM illustrating amplification of light within the active fibers.*

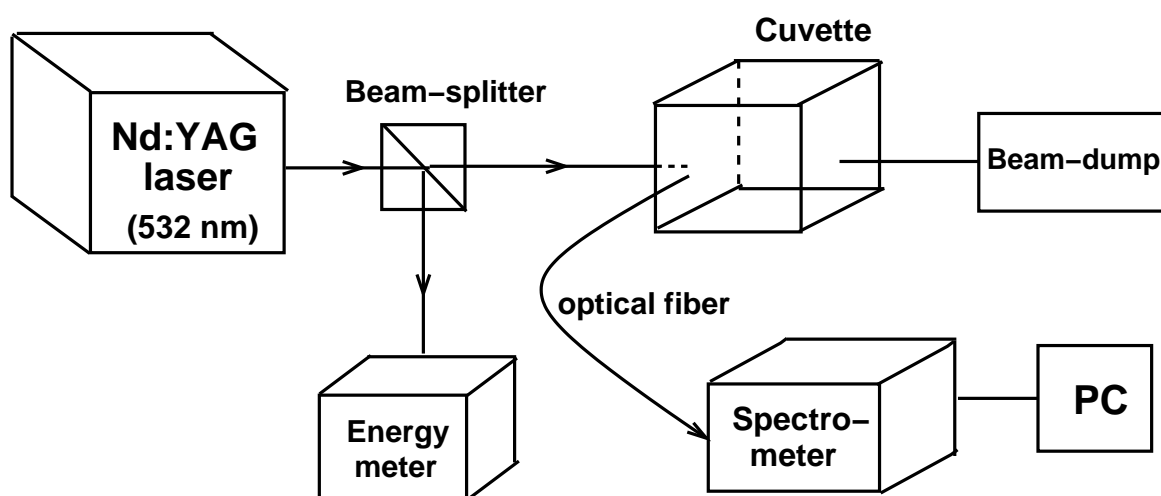


Figure 3: *Schematic of experimental set-up.*

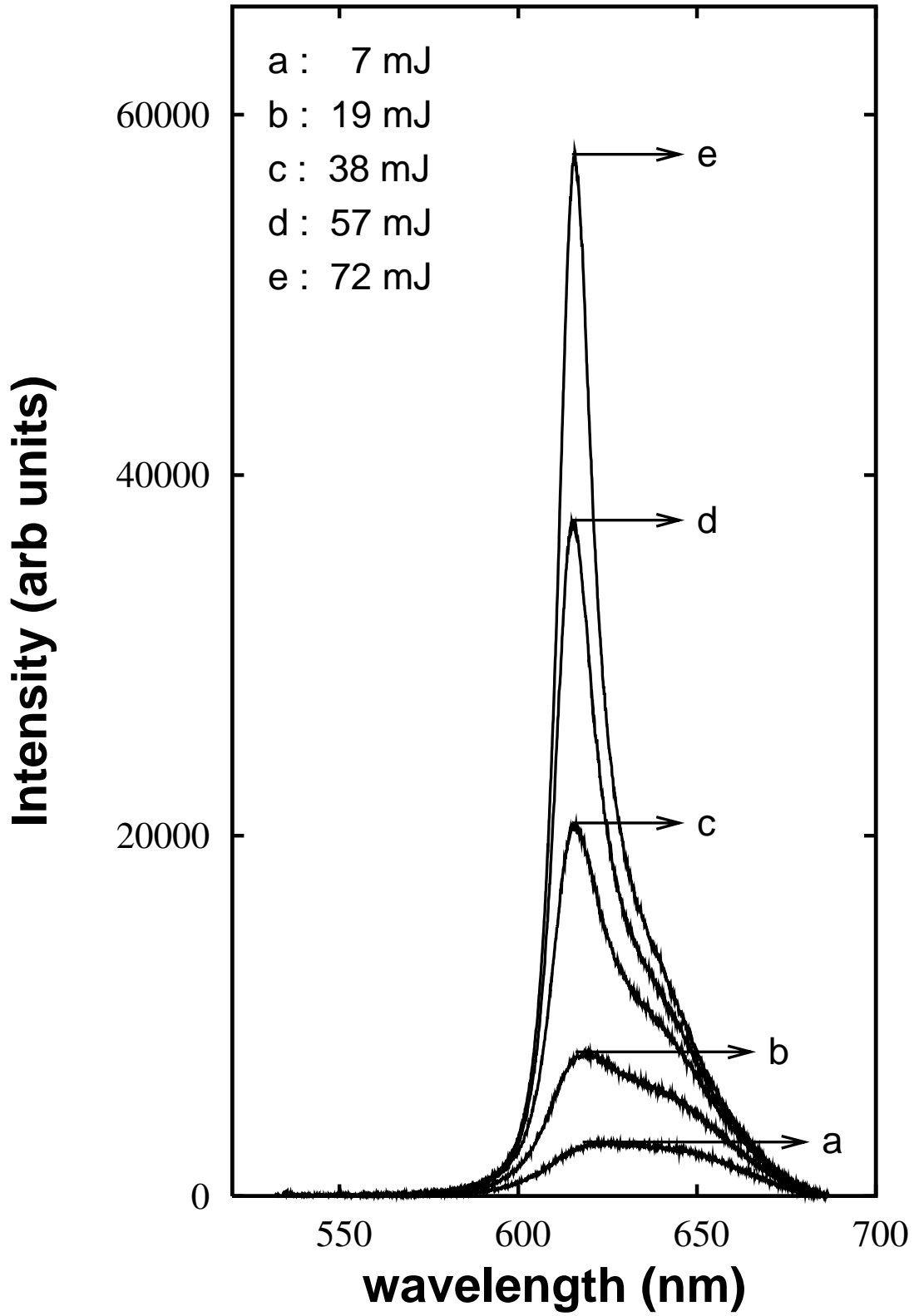


Figure 4: *Gain narrowing with increasing pump powers in an F-RAM made of sub-millimeter pieces of active fiber in water.*

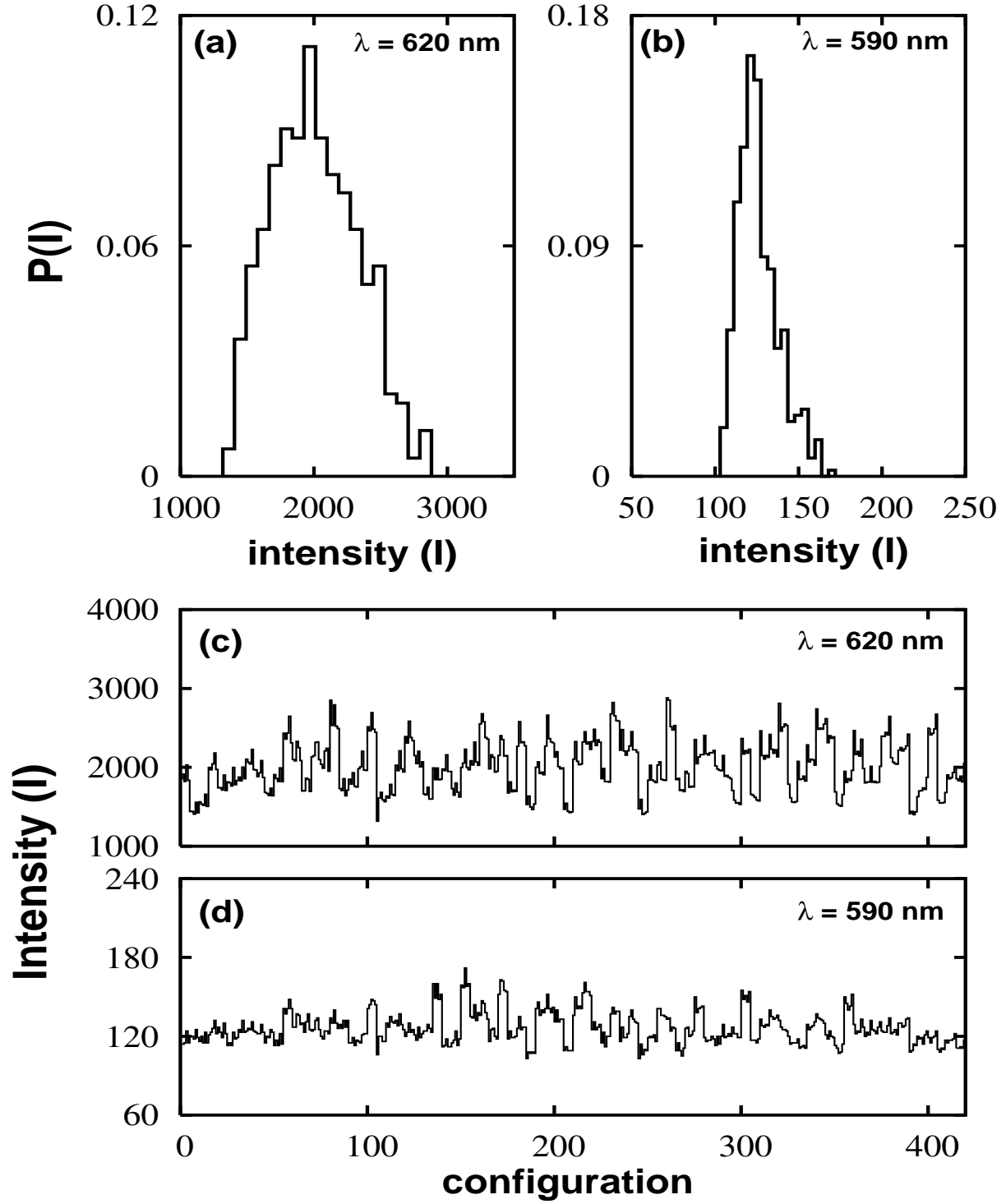


Figure 5: (a),(b) : Histograms of emission at peak and off-peak wavelengths respectively for F-RAM consisting of sub-millimeter pieces of active fiber. (c),(d) : Intensity fluctuations as a function of complexion for the F-RAM at peak and off-peak emission wavelengths.

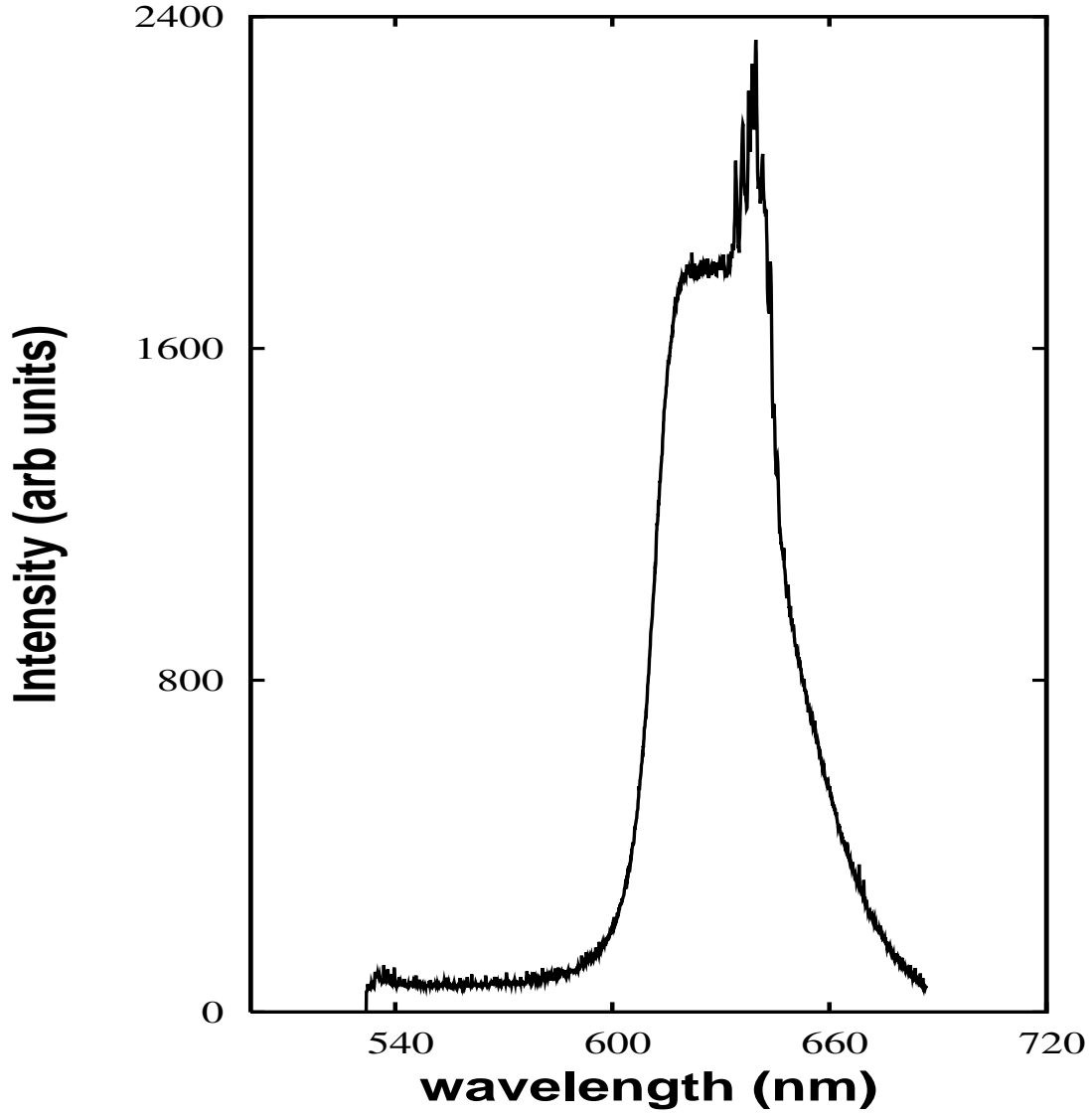


Figure 6: *Typical spectrum of an F-RAM consisting of ten pieces of active fiber of length 6 mm each, embedded in sub-millimeter pieces of active fiber, at pump energy of ~ 26 mJ.*

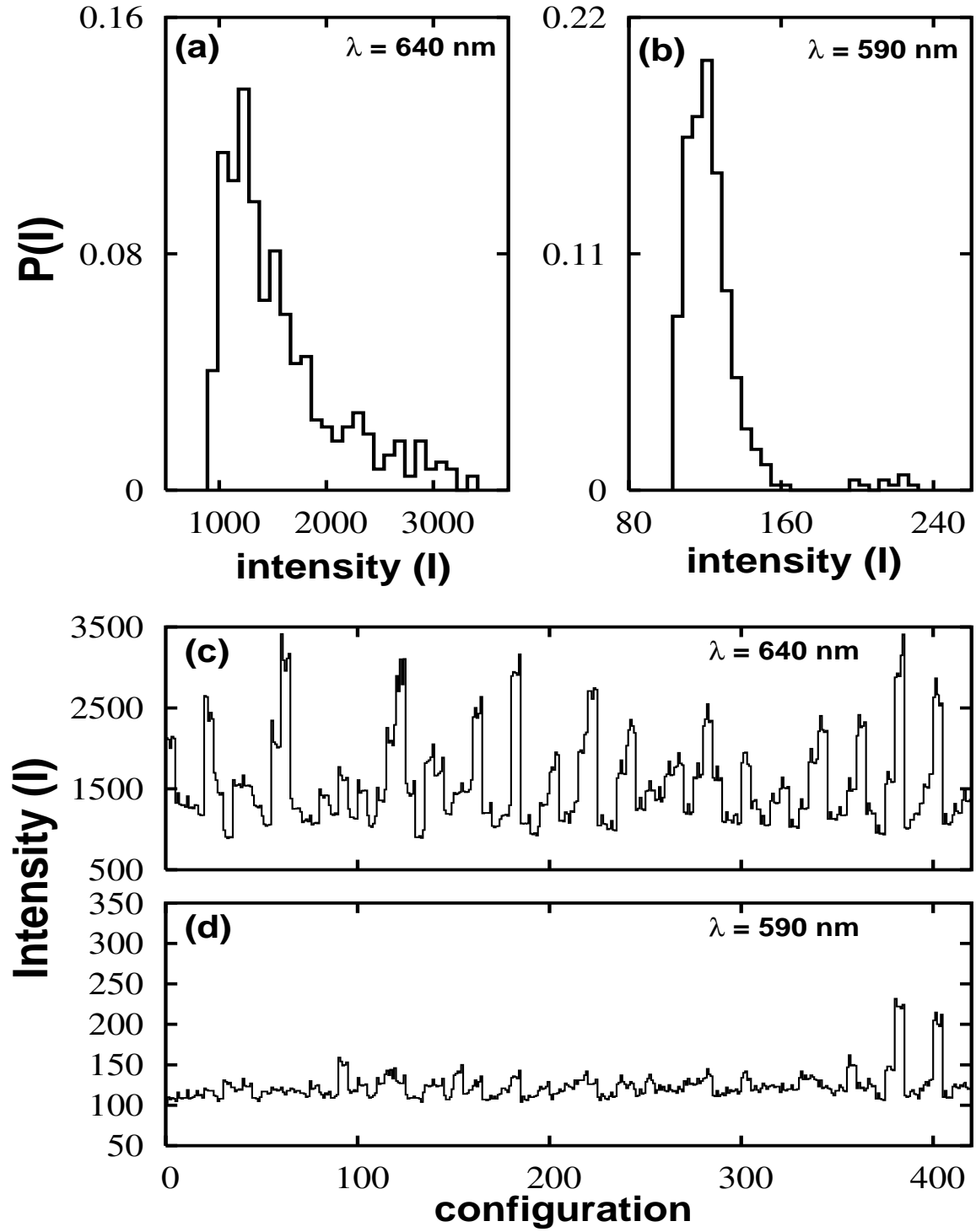


Figure 7: (a),(b) : Histograms of emission at peak and off-peak wavelengths respectively for F-RAM consisting of ten pieces of active fiber of length 6 mm each, embedded in sub-millimeter pieces of active fiber. (c),(d) : Intensity fluctuations as a function of complexion for the F-RAM at peak and off-peak emission wavelengths.

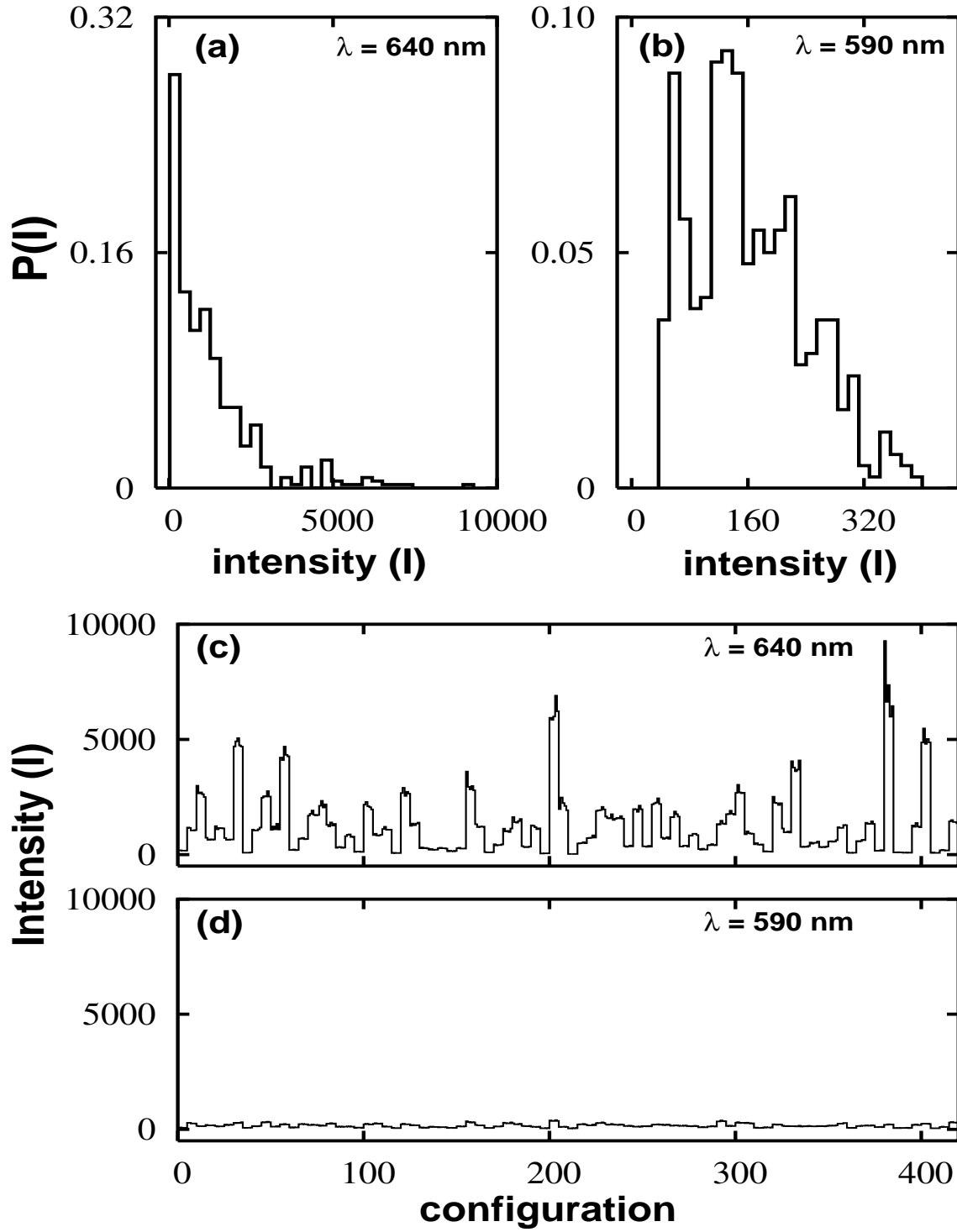


Figure 8: (a),(b) : Histograms of emission at peak and off-peak wavelengths respectively for F-RAM consisting of ten pieces of active fiber of length 6 mm each, in a passive scattering medium made of pieces of non-active white fiber of length ~ 1 mm each. (c),(d) : Intensity fluctuations as a function of complexion for the F-RAM at peak and off-peak emission wavelengths.

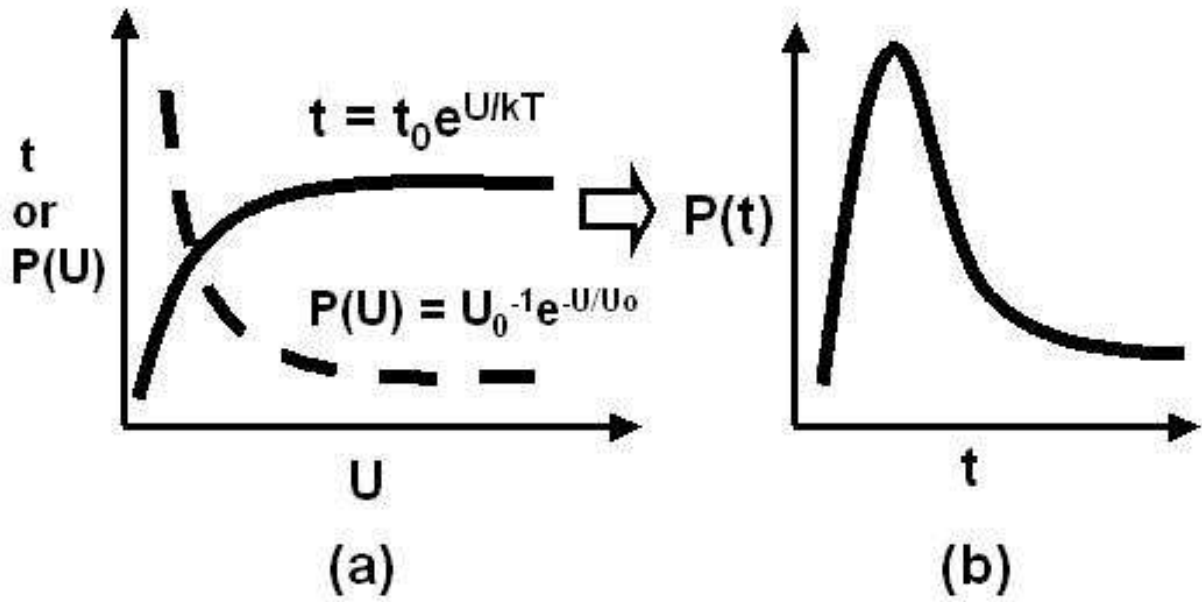


Figure 9: (a) : Distribution of depths of potential wells in an Arrhenius cascade (dotted) and the time of residence in a potential well as function of depth U (solid), (b) : Resulting probability distribution of total time of descent.

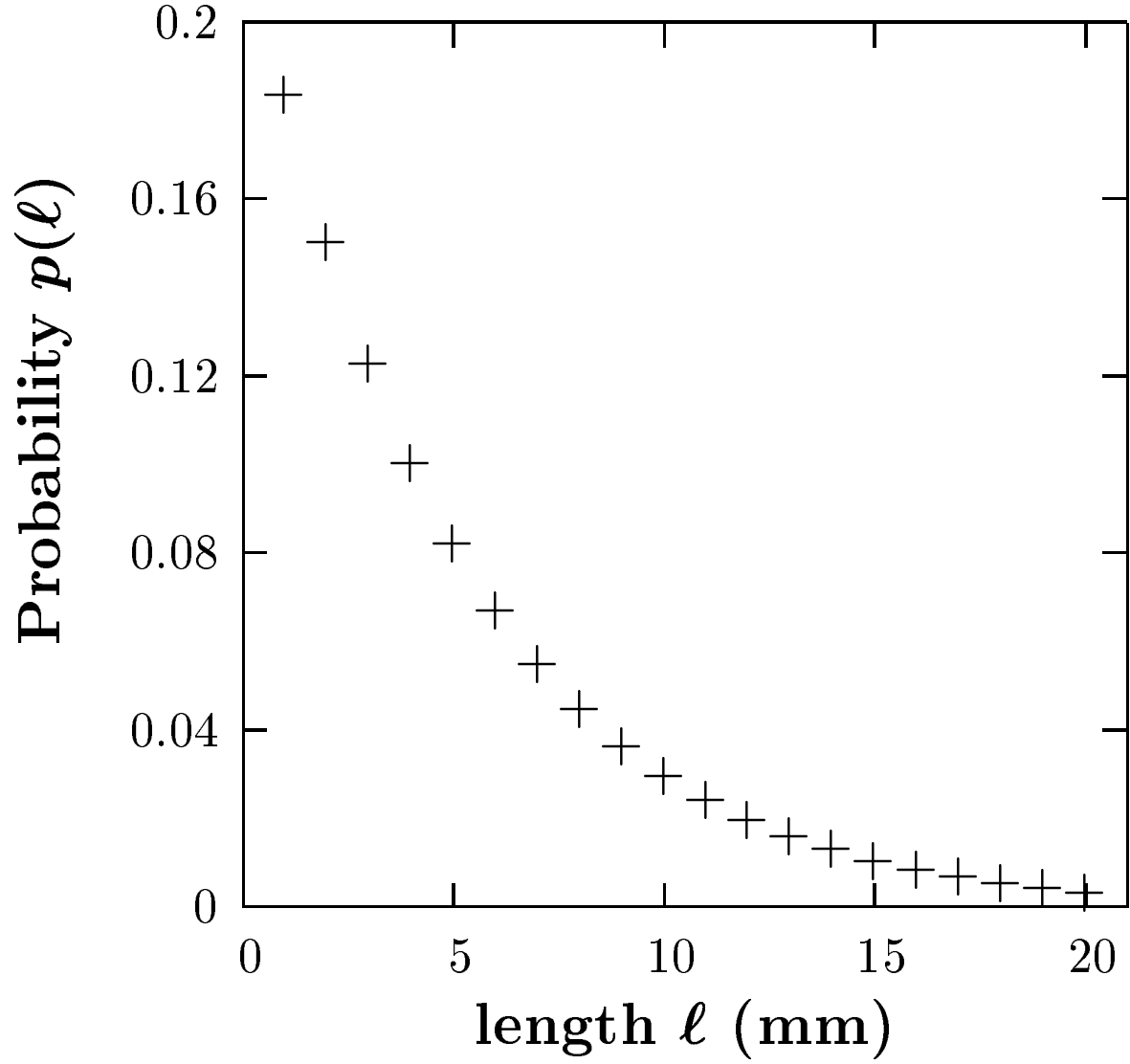


Figure 10: *Probability distribution function for lengths of pieces of active fiber in tailored F-RAM : $\ell_o = 5$ mm.*

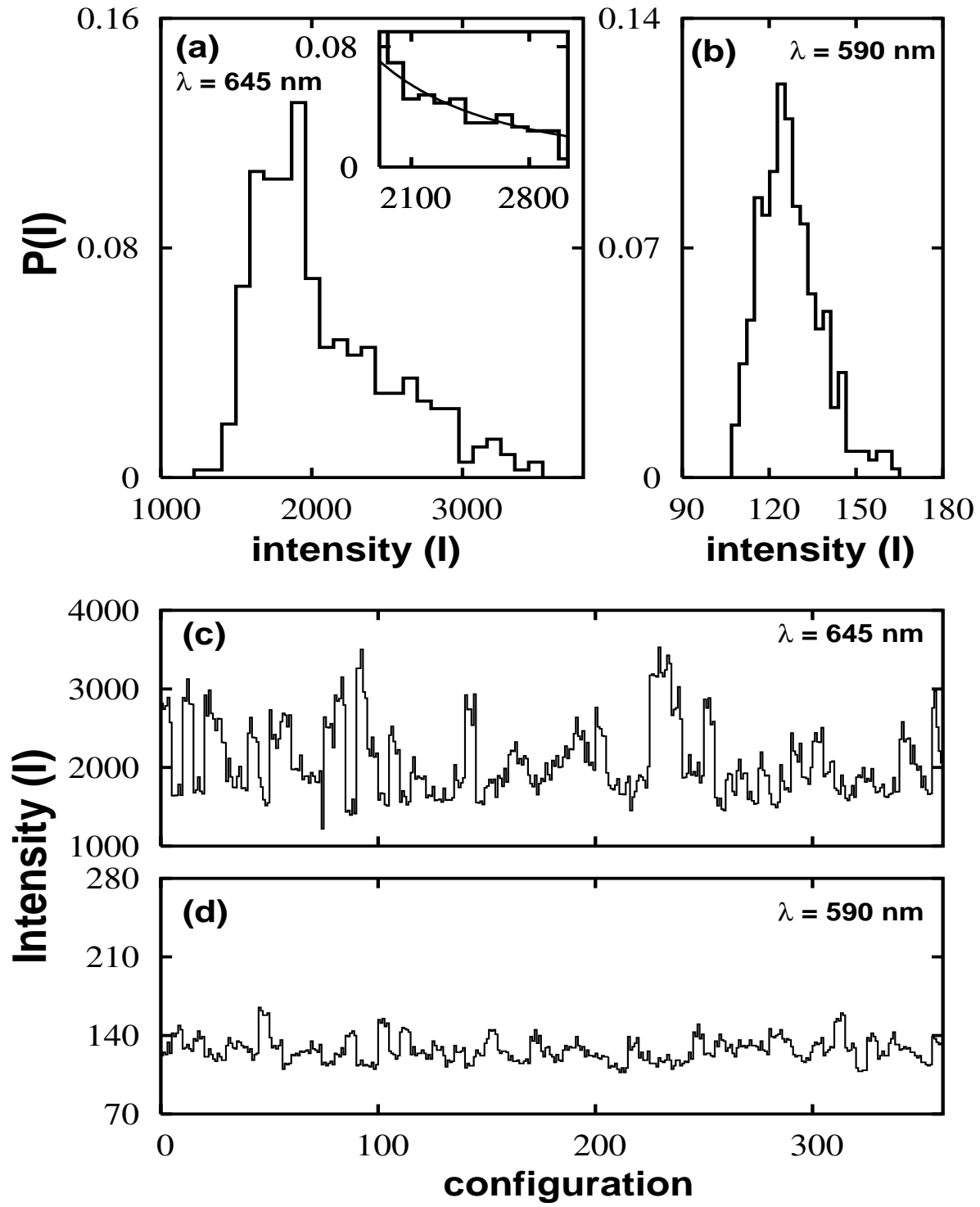


Figure 11: (a),(b) : Histograms of emission at peak and off-peak wavelengths respectively for F-RAM consisting of 350 pieces of active fiber (following exponential distribution for lengths) in a passive scattering medium provided by polystyrene scatterers. (c),(d) : Intensity fluctuations as a function of complexion for the F-RAM at peak and off-peak emission wavelengths.

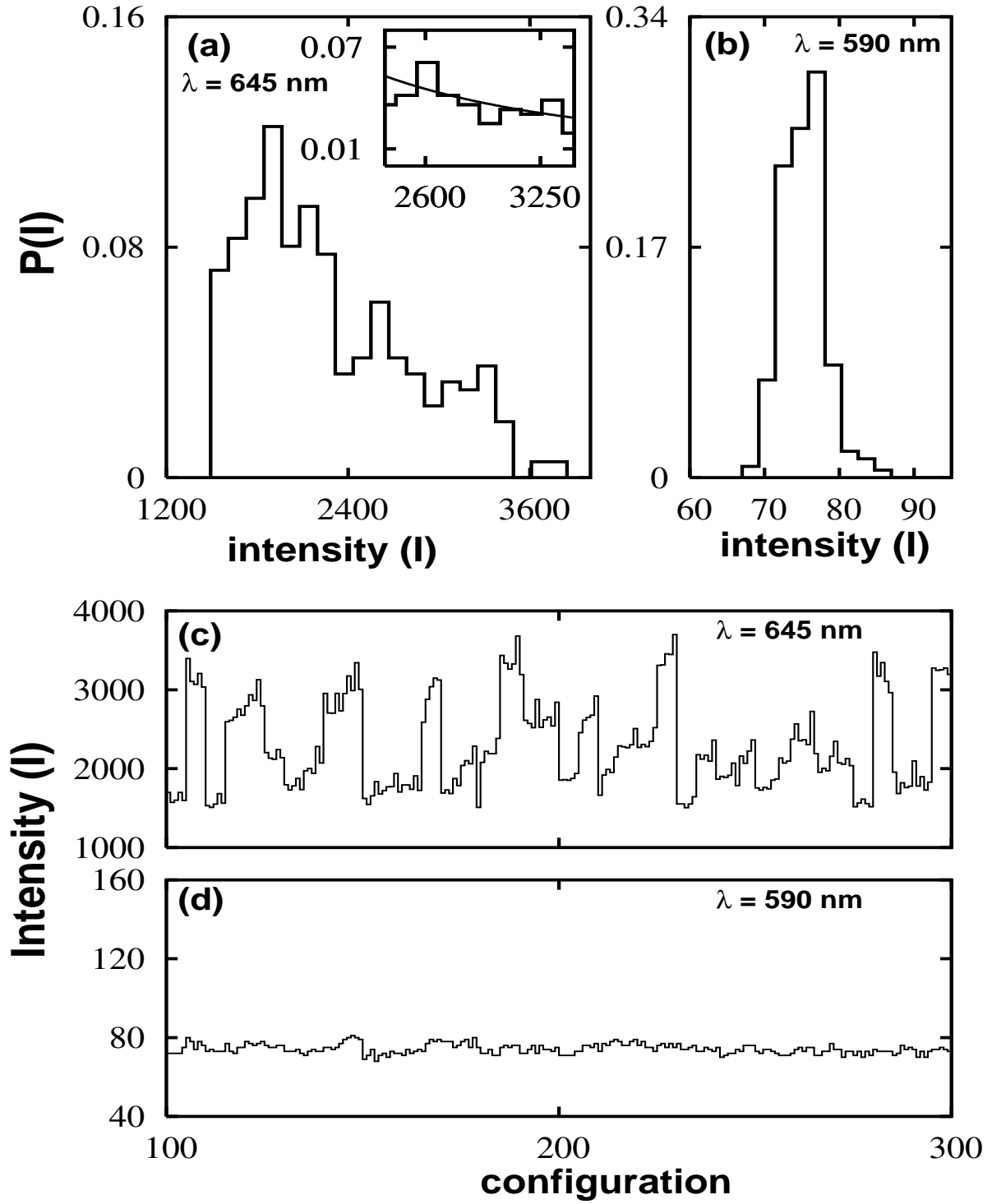


Figure 12: (a),(b) : Histograms of emission at peak and off-peak wavelengths respectively for F-RAM consisting of 800 pieces of active fiber (following exponential distribution for lengths) in a passive scattering medium provided by granular starch. (c),(d) : Intensity fluctuations as a function of complexion for the F-RAM at peak and off-peak emission wavelengths.

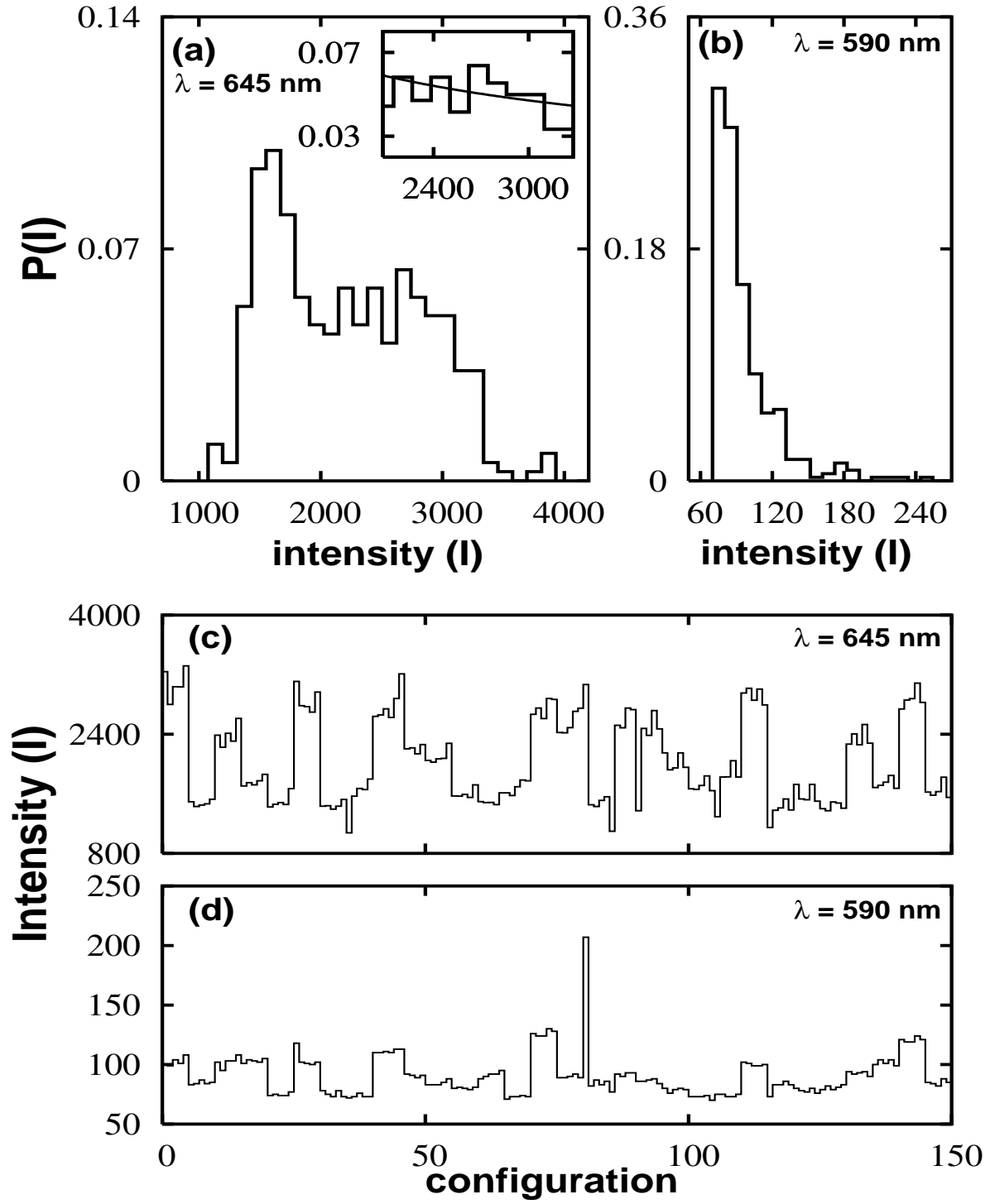


Figure 13: (a),(b) : Histograms of emission at peak and off-peak wavelengths respectively for F-RAM consisting of 800 pieces of active fiber (following exponential distribution for lengths) in a passive scattering medium provided by non-active white fiber pieces (length ~ 1 mm). (c),(d) : Intensity fluctuations as a function of complexion for the F-RAM at peak and off-peak emission wavelengths.

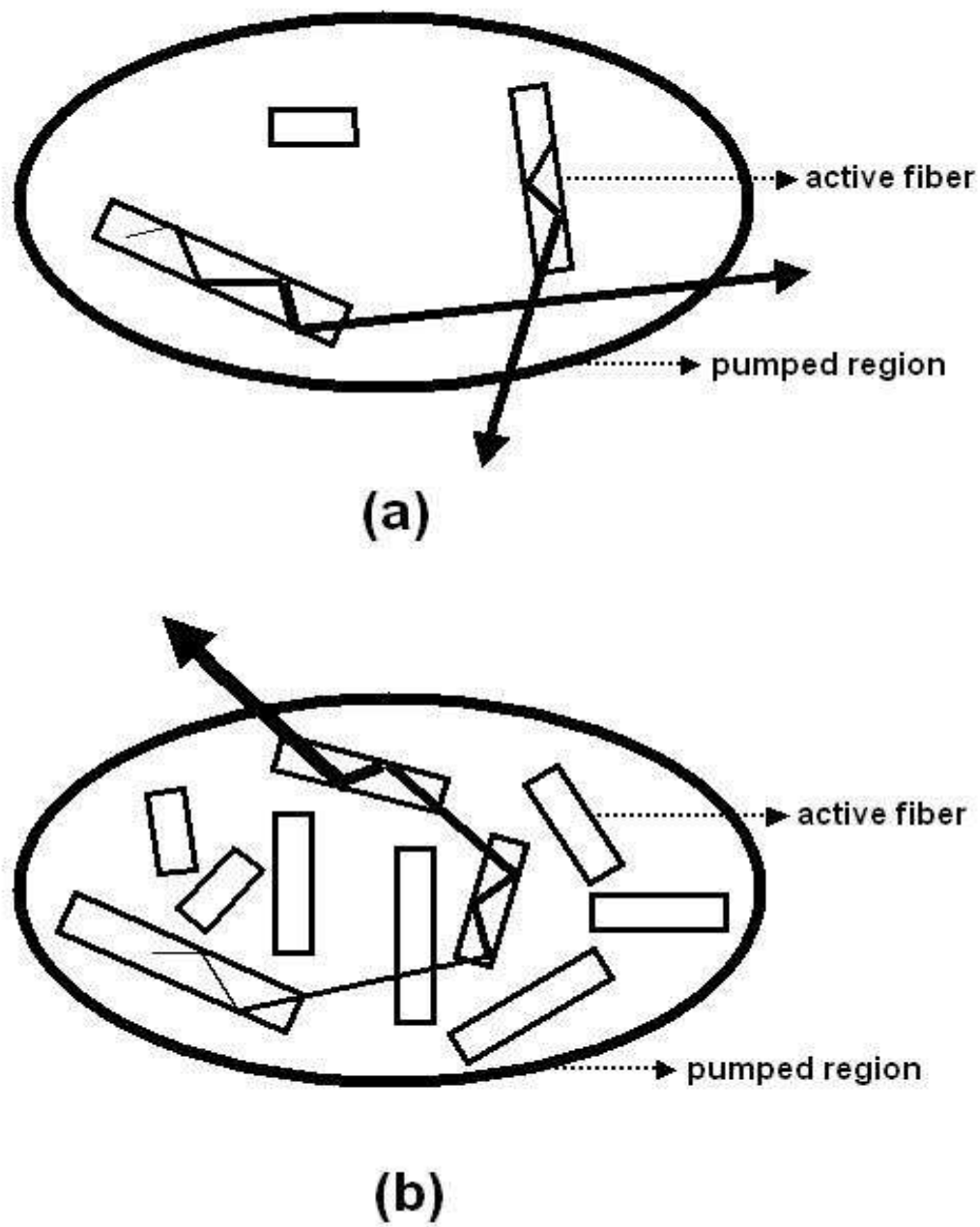


Figure 14: *Schematic of (a) Dilute F-RAM (b) Dense F-RAM*